(1S,2S)-1-(4-Hydroxyphenyl)-2-(4-hydroxy-4-phenylpiperidino)-1-propanol: A Potent New Neuroprotectant Which Blocks *N*-Methyl-D-aspartate Responses

B. L. Chenard,* J. Bordner, T. W. Butler, L. K. Chambers, M. A. Collins, D. L. De Costa, M. F. Ducat, M. L. Dumont, C. B. Fox, E. E. Mena, F. S. Menniti, J. Nielsen, M. J. Pagnozzi, K. E. G. Richter, R. T. Ronau, I. A. Shalaby, J. Z. Stemple, and W. F. White

Central Research Division, Pfizer Inc., Groton, Connecticut 06340

Received March 30, 1995[⊗]

(1S,2S)-1-(4-Hydroxyphenyl)-2-(4-hydroxy-4-phenylpiperidino)-1-propanol (**20**, CP-101,606) has been identified as a potent and selective *N*-methyl-D-aspartate (NMDA) antagonist through a structure activity relation (SAR) program based on ifenprodil, a known antihypertensive agent with NMDA antagonist activity. Sites on the *threo*-ifenprodil skeleton explored in this report include the pendent methyl group (H, methyl, and ethyl nearly equipotent; propyl much weaker), the spacer group connecting the C-4 phenyl group to the piperidine ring (an alternating potency pattern with 0 and 2 carbon atoms yielding the greatest potency), and simple phenyl substitution (little effect). While potent NMDA antagonists were obtained with a two atom spacer, this arrangement also increased α_1 adrenergic affinity. Introduction of a hydroxyl group into the C-4 position on the piperidine ring resulted in substantial reduction in α_1 adrenergic affinity. The combination of these observations was instrumental in the discovery of **20**. This compound potently protects cultured hippocampal neurons from glutamate toxicity (IC_{50} = 10 nM) while possessing little of the undesired α_1 adrenergic affinity (IC_{50} ~ 20 μM) of ifenprodil. Furthermore, **20** appears to lack the psychomotor stimulant effects of nonselective competitive and channel-blocking NMDA antagonists. Thus, **20** shows great promise as a neuroprotective agent and may lack the side effects of compounds currently in clinical trials.

Introduction

A growing body of literature supports the excitotoxin theory of neurodegeneration. Briefly, this theory states that acidic amino acid neurotransmitters (glutamate for example) are aberrantly released in the brain in response to neurodegenerative stimuli.[1] The ensuing hyperactivation of glutamate receptors, in particular the *N*-methyl-D-aspartate (NMDA) class of glutamate receptors, leads to toxic increases in calcium ion influx and neuron death.[2] Many clinical conditions both rapid in onset (stroke for example[3]) and insidiously slow in onset (Alzheimer's disease for example[4]) reveal neuronal cell loss that may be attributable to excitatory amino acid neurotoxicity. Thus, intervention with NMDA antagonists has been proposed as potential therapy for these neurodegenerative conditions.[5]

Antagonism of NMDA receptor function may be effected through interaction at any one of the many modulatory sites of this receptor.[6] Thus, antagonists may be competitive for the glutamate or glycine recognition sites or the polyamine binding site or interact with sites within the channel pore. Examples of each of these classes of antagonists have been reported to inhibit NMDA receptor function in various *in vitro* and *in vivo* models.

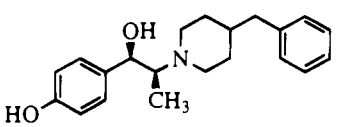

Ifenprodil (**1**)

Our interest in this area originated with the observation that ifenprodil (**1**), an α_1 adrenergic antagonist, also possesses NMDA antagonist activity.[7] This molecule is structurally distinct from any of the known classes of NMDA antagonists and has been suggested to inhibit NMDA receptor function through interactions at the polyamine modulatory site.[8] Ifenprodil possesses nanomolar affinity for several central nervous system (CNS) receptors (α_1, $5HT_{1A}$, $5HT_2$, σ)[9] in addition to NMDA activity, and this lack of selectivity was viewed as undesirable and potentially detrimental for a CNS neuroprotectant. Therefore, the goal of our program was to discover new selective NMDA antagonists with ifenprodil as the lead structure.

In a previous report, we described structural modifications designed to identify the key features of the ifenprodil molecule associated with its NMDA antagonist activity.[9] An observation from that study was that changing the relative stereochemistry from erythro to threo (**2**) resulted in improved NMDA antagonist potency and greatly reduced α_1 affinity. The enhanced selectivity with the threo diastereomer was consistently observed throughout the chemical series. Thus, the present work deals exclusively with threo diastereomers.

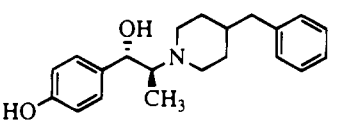

2

In this report, we describe our continuing efforts to refine and enhance the NMDA potency and selectivity of this novel class of glutamate antagonists. This effort has resulted in the identification of (1S,2S)-1-(4-hydroxyphenyl)-2-(4-hydroxy-4-phenylpiperidino)-1-propanol (**20**, CP-101,606), a compound which possesses an

[⊗] Abstract published in *Advance ACS Abstracts*, July 1, 1995.

0022-2623/95/1838-3138$09.00/0

Scheme 1[a]

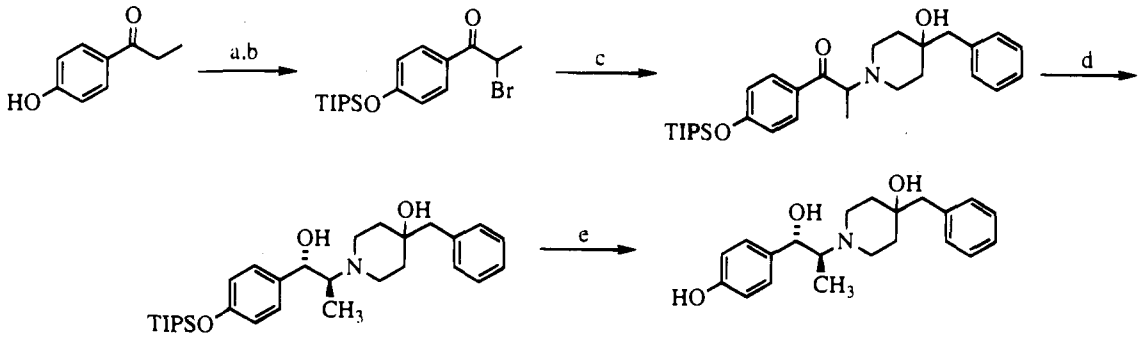

[a] (a) TIPSCl, imidazole, DMF; (b) Br_2, CCl_4; (c) 4-hydroxy-4-phenylpiperidine, Et_3N, ethanol, Δ; (d) $NaBH_4$, ethanol; (e) Bu_4NF, THF.

excellent potency/selectivity profile for development as an antineurodegenerative agent.

Chemistry

The synthesis of compounds **1**–**4** has been described.[10] New compounds **5**–**21** were prepared in a similar fashion (Scheme 1).[11] Briefly, 4-hydroxypropiophenone was protected as its triisopropylsilyl ether[12] and brominated with elemental bromine in carbon tetrachloride. The α-bromo ketone was coupled with commercial 4-hydroxy-4-benzylpiperidine or a related piperidine derivative. The resulting ketone was reduced with sodium borohydride in ethanol. Finally the phenol was unmasked with tetrabutylammonium fluoride. Two steps in the sequence deserve further comment. First, the bulky (triisopropylsilyl)phenol protecting group generally afforded higher product yields than smaller silyl ethers. Less bulky groups including *tert*-butyldimethylsilyl were found to be partially removed during both the coupling and reduction steps. Second, high threo diastereomeric selectivity (generally about 10:1) could be achieved via addition of the ketone to an ethanol slurry of sodium borohydride. In contrast, related borohydride reductions carried out under acidic conditions have been reported to give erythro selective reductions.[13]

The chain extended piperidines were prepared in a straightforward manner from *N*-CBZ-4-piperidone by Grignard addition in ether and hydrogenolysis (eq 1). This sequence provided usable quantities of the required intermediates, but the Grignard addition was sometimes problematic as pinacol-like coupling through reduction of the piperidone was always a byproduct of the reaction and actually became the major reaction pathway when the addition was carried out in tetrahydrofuran.

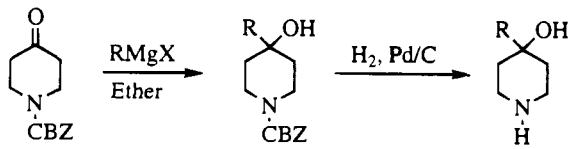

Eq. 1

In Vitro Pharmacology

Since the compounds described herein do not interact with any of the well-characterized NMDA modulatory sites, a functional measure of NMDA antagonist activity was employed. Specifically, the potency was measured for inhibition of glutamate-induced neuron death in primary cultures of rat hippocampal neurons.[14] Glutamate toxicity in this cell culture model has been linked to stimulation of NMDA receptors, and all known classes of NMDA antagonist are efficacious in the assay.

A prime objective in our program was to develop an NMDA antagonist with minimal interaction at other receptors. As noted above, ifenprodil has nanomolar affinity at several receptors. For our initial screening, we focused on elimination of α_1 adrenergic affinity since interaction at this receptor is responsible for ifenprodil's antihypertensive effect in humans.[15] We measured α_1 affinity with a standard binding assay using [^{3}H]-prazosin as the radioligand.[16] The ratio of α_1 affinity/neuroprotection was used as an index of selectivity.

Results and Discussion

In our previous report we examined structural modifications of ifenprodil-seeking compounds with an enhanced potency/selectivity profile.[9] Not surprisingly, several changes detrimental to NMDA receptor antagonism were noted. The most intriguing of these negative changes was that replacement of C-4 of piperidine with nitrogen [piperazine (**3**)] resulted in complete loss of NMDA antagonist activity. Since this change would not result in any steric perturbation in the active site, it seemed reasonable that an auxiliary binding interaction (either dipolar or hydrogen bonding) may be present near this region of the molecule. Accordingly, further structural changes were introduced in the vicinity of C-4 of the piperidine ring seeking to capitalize on this putative interaction. While piperazine **3** and amide **4** were essentially inactive, incorporation of a hydroxyl group at C-4 resulted in a very potent compound **5** with $IC_{50} = 58$ nM in the cell culture neuroprotection model. Additionally, this modification reduced α_1 binding affinity to greater than 10 μM. Conversion of the C-4 hydroxyl group to a methyl ether (**6**) resulted in complete loss of NMDA antagonist activity. Comparison of compounds **2** and **5** (Table 1) suggests that the piperidine C-4 hydroxyl group improved the selectivity profile of **5** by substantially reducing α_1 adrenergic binding affinity.

The SAR of this new structural series was carefully explored to optimize NMDA activity (Table 1). To begin, the pendent methyl group was manipulated (**5** and **7**–**9**). Replacement with hydrogen or ethyl resulted in nearly equipotent compounds. However, extension to a propyl group substantially reduced potency. None of these changes returned any level of α_1 affinity. It is particularly interesting that removal of the methyl group (**7**) did not result in enhanced α_1 affinity since this change removes the diastereomeric control of receptor selectivity noted previously.[9] Clearly the piperidine C-4 hydroxyl group defines a second powerful receptor

Table 1. Neuroprotection in Cell Culture versus α_1 Adrenergic Affinity

compd	structure	neuroprotection[a] IC_{50} ± SEM, nM (*n*)	α_1[a] IC_{50} ± SEM, nM (*n*)	selectivity ratio[b]
1	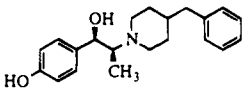	263 ± 63 (4)	100 ± 36 (5)	0.38
2	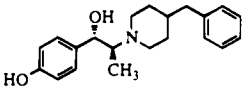	55 ± 13 (3)	843 ± 137 (3)	15.3
3	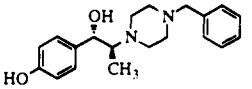	10 000 (4)	4633 ± 2056 (3)	NM
4	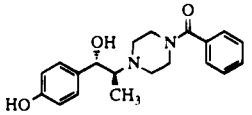	>10 000 (2)	>10 000 (2)	NM
5	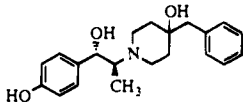	58 ± 17 (4)	>10 000 (2)	>172
6	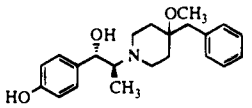	>10 000 (2)	not tested	NM
7	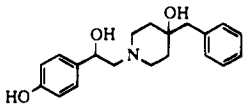	63 ± 22 (3)	>10 000 (2)	>158
8	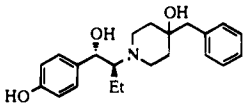	68 ± 16 (3)	>10 000 (2)	>147
9	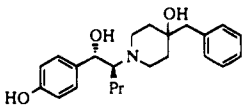	1300 ± 400 (3)	>10 000 (2)	7.7
10	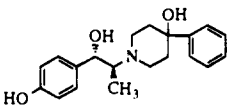 CP-98,113	10.2 ± 2.2 (14)	5700 ± 1191 (4)	559
11	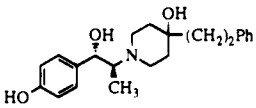	1.3 ± 0.5 (3)	137 ± 119 (3)	105
12	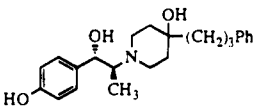	15.7 ± 3.9 (3)	2350 (2)	150
13	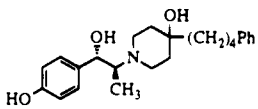	1000 (2)	2300 (2)	2.3
14	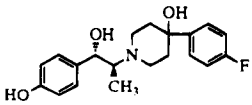	4.0 ± 2.5 (3)	2700 ± 556 (3)	675
15	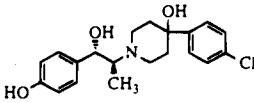	2.0 ± 0.63 (3)	1480 (2)	740
16	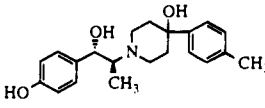	2.7 ± 0.82 (3)	2166 ± 461 (3)	1083
17	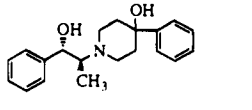	>1000 (2)	>10 000	NM

Table 1 (Continued)

compd	structure	neuroprotection[a] IC_{50} ± SEM, nM (*n*)	α_1[a] IC_{50} ± SEM, nM (*n*)	selectivity ratio[b]
18	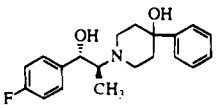	>1000 (2)	6900 (2)	NM
19	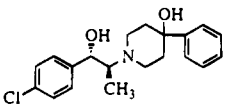	>1000 (2)	3133 ± 1250 (3)	NM
20	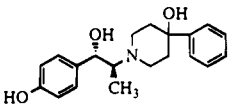 (+) CP-101,606	11 ± 4.3 (3)	19 520 ± 11 700 (5)	1774
21	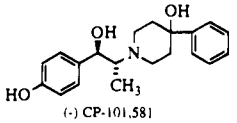 (-) CP-101,581	11 ± 2 (3)	8450 ± 4780 (6)	768

[a] Average of two experiments for values of 1000 or more unless otherwise stated. [b] NM = not meaningful.

selectivity control element which may work in concert with or in the absence of the diastereomeric influence.

The length of the tether between the phenyl and piperidine rings further refined the SAR (**5** and **10**–**13**). Removal of the methylene spacer yielded **10** (CP-98,113), a compound with 6-fold greater potency (IC_{50} = 10 nM) as an NMDA antagonist with little change in α_1 affinity (IC_{50} = 6 μM). Extension of the spacer to two carbons yielded the most potent NMDA antagonist of the series, **11** (IC_{50} = 1.3 nM). Unfortunately the two-atom spacer returns significant α_1 affinity to the molecule (IC_{50} = 137 nM). Further extension to a three-carbon spacer, **12**, retains excellent NMDA antagonist potency, and the α_1 affinity is lost again. Only when the carbon chain is extended to four atoms does the NMDA activity drop off to the micromolar range. Thus the phenyl ring appears to fit into a rather deep pocket estimated to be up to 10 Å from C-4 of the piperidine ring by inspection of Dreiding models. Favorable binding, presumably through a π stacking interaction,[9] may be attained almost anywhere within this pocket. Based on potency and selectivity considerations, further definition of the SAR was carried out with the phenyl ring directly attached to C-4 of the piperidine ring.

Substitution in the 4-position of the phenyl ring was well tolerated (**10** and **14**–**16**). Both electron-donating and -withdrawing groups retained excellent potency and selectivity. It may be assumed that these substituents extend out into the 10 Å pocket defined above.

Finally, phenolic hydroxyl replacements were examined (**10** and **17**–**19**). In the previous study of ifenprodil-related compounds, it was observed that fluorine was a suitable replacement for the hydroxyl.[9] In fact, Synthelabo has selected a chloro derivative of ifenprodil, eliprodil (SL 82.0715), for development for the treatment of stroke.[17] However, for the present series, halogen was unsuitable as a hydroxyl surrogate: both the fluorinated and chlorinated derivatives (**18** and **19**, respectively) as well as the proteo analog **17** had NMDA antagonist activity in the micromolar range.[18]

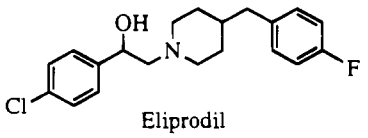
Eliprodil

From the SAR developed above, **10** was identified as a compound with potent NMDA antagonist activity and the desired separation of α_1 adrenergic binding affinity. In preparation for further advancement, **10** was profiled in several binding assays to assess affinity at other CNS neurotransmitter and neuromodulatory sites. Compound **10** was found to be highly selective for the NMDA receptor with >1 μM affinity for dopamine (D_1, D_2), serotonin ($5HT_{1A,D}$, $5HT_{2A,C}$, $5HT_3$), acetylcholine (muscarinic and nicotinic), $GABA_A$, opiate, histamine (H_1, H_2), AMPA, or kainate receptors. Only σ binding was appreciable with IC_{50} = 60 nM. In addition, **10** had no appreciable affinity (>1 μM) for the competitive NMDA site, the ion channel site labeled by TCP, or the strychnine-insensitive glycine site.

The NMDA receptor modulatory site through which **10** acts is presently unknown, although ifenprodil has been suggested to act at the polyamine site.[8] It is possible that **10** is selective for a subtype of NMDA receptor. One observation which supports this possibility is the variable degree of neuroprotection-afforded neurons from different brain regions in response to a glutamate challenge.[19] While **10** protects hippocampal neurons with IC_{50} = 10 nM, little protection was observed in cerebellar granule cell cultures (IC_{50} > 10 000 nM). Further work to define the mode of action of **10** at the NMDA receptor is in progress.

Resolution Studies

Two methanol recrystallizations of **10** with (−)-tartaric acid gave enantiomerically pure (+)-**20** (CP-101,606). The mother liquors were neutralized and treated with (+)-tartaric acid to yield the pure (−)-antipode **21** (CP-101,581). Enantiomeric purity was assessed by NMR (500 MHz) using the chiral shift reagent (*R*)-(−)-2,2,2-trifluoro-1-(9-anthryl)ethanol. Because of the low solubility of the free base, CD_3CN was used for the experiment. The benzylic proton α to the hydroxyl group appeared as a pair of doublets (overlapping but fully resolved) in the region from δ 4.05 to 4.15 for the racemic material. Thus, optical purity was estimated to be greater than 98%. HPLC with a chiral column[20] provided a second measure of enantiomeric purity. Under these conditions no evidence of contamination with the opposite enantiomer was observed in purified samples of **20** or **21**.

Table 2. *In Vivo* Activity of CP-101,606 (**20**) and CP-101,581 (**21**)

study	CP-101,606 (**20**)	CP-101,581 (**21**)
blockade of haloperidol-induced catalepsy, ED_{50} rat, sc	0.4 ± 0.2 mg/kg	0.5 ± 0.3 mg/kg
antagonism of NMDA-stimulated fos induction, ED_{50} mouse, ip	1.0 mg/kg (0.3–5)[a]	5.0 mg/kg (2.8–9.1)

[a] 95% confidence interval.

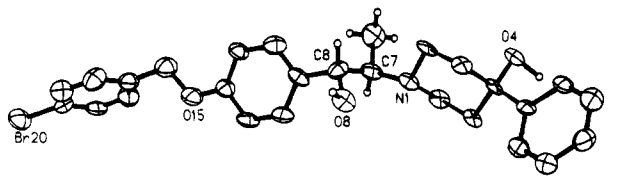

Figure 1. X-ray structure of the *p*-bromobenzyl ether of **21**.

The phenolic hydroxyl group of **21** was converted to a crystalline 4-bromobenzyl ether. X-ray structural analysis defined the absolute stereochemistry of this enantiomer as 1*R*,2R (as shown in Table 1). Thus, the absolute stereochemistry of **20** was 1*S*,2*S* (see Figure 1). *In vitro* activities of **20** and **21** may be compared to the racemate **10** in Table 1. From these data it is clear that the enantiomers are nearly equipotent as NMDA antagonists but the (+)-enantiomer possesses slightly less affinity for the α_1 receptor. That both enantiomers of **10** have similar NMDA antagonist activity is not surprising as this relative lack of "stereosensitivity" was observed for the threo enantiomers of ifenprodil [only a 3× selectivity favoring the (−)-enantiomer]. Neither antipode showed a decided advantage over the other or the racemate *in vitro*.

In Vivo Studies

Functional effects of NMDA antagonists have been observed in a variety of animal models. We initially evaluated compounds for their ability to block haloperidol-induced catalepsy in rats, a model for Parkinson's disease.[21] This procedure allowed relatively easy assessment of CNS activity after peripheral administration (sc) of test compounds. The assay was rapid and readily amenable to dose–response measurements. Enantiomers **20** and **21** were both potent at blocking haloperidol-induced catalepsy and indistinguishable with ED_{50}s less than 1 mg/kg (Table 2).

The immediate early gene, *cfos*, is induced in the CNS in response to a wide variety of stimuli,[22] including in response to CNS injury[23] and excitotoxins which cause neuron loss (such as kainic acid,[24] NMDA,[25] and quinolinic acid[26]). NMDA antagonists have been reported to prevent *cfos* induction following activation of the NMDA receptor.[23,25,26] Thus, prevention of NMDA-induced *cfos* expression may be used as an *in vivo* measure of NMDA antagonist activity.

We examined the ability of **20** and **21** (ip) to block NMDA (ip) stimulated *cfos* induction in mice (Table 2). In this assay **20** was effective at 1 mg/kg (ED_{50}), similar to its activity in the haloperidol-induced catalepsy paradigm. In contrast, **21** was somewhat less effective (ED_{50} = 5 mg/kg), suggesting the two enantiomers may be differentially effective in this measure.[27]

Conclusions

The large number of patients suffering from neurodegenerative conditions, the general lack of effective treatments, and the potential utility of NMDA antagonists to afford such a treatment has been the impetus for extensive exploration of NMDA antagonists as therapeutic agents. Unfortunately, problems with side effects have hindered development of competitive antagonists and channel-blocking agents.[28] Ifenprodil and related compounds do not interact with the NMDA receptor through any of the well-defined sites and may not be subject to the same liabilities of previously described antagonists. However, the relatively weak NMDA antagonist potency and nanomolar affinity for several CNS receptors of the known members of this class present a distinct set of challenges to overcome. In this study, the SAR of ifenprodil was investigated to discover more potent and selective NMDA antagonists. We have defined the importance of the pendent methyl group and the spacer group connecting the phenyl ring to C-4 of the piperidine ring. In addition, a receptor selectivity controlling hydroxyl group was introduced at C-4 of the piperidine ring. The C-4 hydroxyl was incorporated based on the substantial reduction in NMDA antagonist action of the related piperazine analog **3**. The selectivity control of the C-4 hydroxyl was apparent throughout the series of analogs in Table 1 with the notable exception of compound **11**. The two carbon spacer overrides the selectivity control of the C-4 hydroxyl as well as that due to threo relative stereochemistry.[29] From this SAR study, **10** had an excellent potency/selectivity profile. The enantiomers of **10** were prepared, and study of their pharmacological properties showed both to be potent and selective agents. On the basis of *in vitro* and *in vivo* activity at NMDA receptor-mediated responses, lack of α_1 adrenergic receptor affinity (*in vitro* binding), lack of other CNS receptor interactions as noted above, and other measures of neuroprotection which will be reported elsewhere, we have selected **20** for further development.

An issue which remains to be addressed is the mechanistic basis for NMDA antagonist activity observed with these compounds. It has previously been suggested that ifenprodil compounds interact with the NMDA receptor through a polyamine modulatory site,[8] a conclusion which we did not support based on our neuroprotection studies in hippocampal cell cultures.[14] A more recent study suggests that the site of brain tissue used in the culture (cortex versus hippocampus) may influence the sensitivity of the polyamine site to ifenprodil.[19]

It is now believed that the NMDA receptor is a heteromeric pentamer requiring at least one NMDAR1 subunit and one or more of the NMDAR2 subunits.[30] Although distinct regional distributions of NMDA receptor subunits have been reported (based on mRNA distributions),[31] the precise makeup of NMDA receptors in any particular tissue is unknown. Thus, it is likely that the NMDA receptor is in fact a heterogeneous family of receptors differentially expressed in different brain regions and possibly even within the same region. Heterogeneity within the NMDA receptor family could also account for the apparent differences in the actions of ifenprodil in different brain regions. Specifically, ifenprodil has been reported to interact selectively with the NMDAR2B subunit expressed in the forebrain.[32]

The highly potent and effective neuroprotection afforded by **20** in neurons cultured from forebrain but not cerebellum suggests that this compound also displays similar NMDA receptor subunit selectivity. However, until more definitive studies are carried out with cloned NMDA receptor subtypes, it is inappropriate to draw any conclusions regarding the mode of action of ifenprodil or our compounds at NMDA receptors.

In conclusion, **20** functions as a forebrain-selective NMDA antagonist with minimal interaction at other CNS receptors. It has no stimulant or psychotomimetic liability and does not appear to interfere with memory processes.[33] Drug metabolism studies indicate that the compound efficiently partitions into the brain after peripheral administration (iv).[33] Thus, with substantially improved potency, good brain penetration, and an improved safety profile, the full range of potential clinical utility of this class of compounds will be explored.

Experimental Section

General Procedures. Melting points were taken with a Thomas-Hoover melting point apparatus and are uncorrected. Infrared spectra were recorded on Perkin-Elmer 283B or 1420 spectrophotometers in chloroform solution unless otherwise stated and are reported in reciprocal centimeters. Infrared spectra of KBr pellets were recorded on a Nicolet 510 FT-IR by the diffuse reflectance method (DRIFTS). Only strong bands are reported unless otherwise stated. Proton NMR were obtained at 250 or 300 MHz with Bruker AM 250 or AM 300 or Varian XL-300 instruments. NMR data are reported in parts per million (δ) and are referenced to the deuterium lock signal from the sample solvent (deuteriochloroform, unless otherwise stated). Optical rotations were determined with a Perkin-Elmer 241 MC polarimeter. Elemental analyses were determined by our own analytical group. Tetrahydrofuran was distilled from sodium benzophenone ketyl immediately prior to use. All reactions were carried out under a nitrogen atmosphere and were stirred magnetically unless otherwise specified.

Compounds **5**–**21** were all prepared by essentially the same procedure (Scheme 1). The sequence is illustrated for **10**, followed by analytical data for **5**–**9** and **11**–**21**.

α-Bromo-4-[(triisopropylsilyl)oxy]propiophenone. Imidazole (124 g, 2 mol) and 4-hydroxypropiophenone (120 g, 0.8 mol) were dissolved in DMF (300 mL), and triisopropylsilyl chloride (200 g, 1.04 mol) was added dropwise. The mixture was stirred 3 h; then it was poured onto water (4 L). The solution was extracted with ether (4 × 1.5 L) and the combined organic phase was washed with 1 N aqueous lithium chloride (3 × 1 L). The organic layer was dried over calcium sulfate and concentrated at reduced pressure. All volatiles were removed by Kugelrohr distillation (100–110 °C pot temperature, 0.1 mm), leaving behind 243.2 g (99%) of 4-[(triisopropylsilyl)oxy]propiophenone as a clear yellow oil: NMR ($CDCl_3$) δ 7.79 (d, J = 8.5 Hz, 2 H), 6.81 (d, J = 8.5 Hz, 2 H), 2.87 (q, J = 7 Hz, 2 H), 1.25–1.11 (m, 6 H), 1.03 (d, J = 7 Hz, 18 H). This ketone was dissolved in carbon tetrachloride (4.5 L) in a three-necked flask equipped with mechanical stirrer and addition funnel. Bromine (40.8 mL, 0.79 mol) in carbon tetrachloride (500 mL) was added dropwise over 1.5 h (generally a small portion of the bromine solution was added and allowed to stir until the reaction initiated, usually within 15 min). The bromine color dissipated essentially on contact with the solution. The mixture was allowed to stir 1.5 h more, and then the HBr was removed from the solution with a stream of nitrogen. The HBr gas was trapped by bubbling the effluent nitrogen gas through a stirred 1.2 N sodium hydroxide solution (700 mL). The reaction mixture was washed with water (2×), saturated aqueous bicarbonate, water, and brine; then it was dried through phase separating paper and concentrated at reduced pressure to yield 304.2 g (100%) of the product as a light brown oil: NMR ($CDCl_3$) δ 7.94 (d, J = 9 Hz, 2 H), 6.91 (d, J = 9 Hz, 2 H), 5.24 (q, J = 6.5 Hz, 1 H), 1.87 (d, J = 6.5 Hz, 3 H), 1.33–1.17 (m, 3 H), 1.10 (d, J = 7 Hz, 18 H). This material was used without further purification and could be stored at 0 °C for at least 6 months without noticeable decomposition.

1-[4-[(Triisopropylsilyl)oxy]phenyl]-2-(4-hydroxy-4-phenylpiperidino)-1-propanone. A solution of 4-hydroxy-4-phenylpiperidine (11 g, 62.1 mmol), α-bromo-4-[(triisopropylsilyl)oxy]propiophenone (24 g, 62.3 mmol), and triethylamine (17.3 mL, 124 mmol) in ethanol (1 L) was refluxed overnight (16 h). The reaction was concentrated directly onto silica gel and chromatographed. Elution with 10%, 25%, and finally 50% ethyl acetate/hexane gave 23.17 g (78%) of the product as an orange oil: NMR ($CDCl_3$) δ 8.03 (d, J = 8.5 Hz, 2 H), 7.47 (d, J = 8.5 Hz, 2 H), 7.33 (t, J = 7.5 Hz, 2 H), 7.26–7.24 (m, 1 H), 6.89 (d, J = 8.5 Hz, 2 H), 4.08 (q, J = 7.5 Hz, 1 H), 2.90–2.60 (m, 2 H), 2.25–2.10 (m, 2 H), 1.85–1.75 (m, 2 H), 1.65–1.55 (m, 2 H), 1.32–1.22 (m, 6 H), 1.10 (d, J = 7 Hz, 18 H); IR ($CHCl_3$) 2940, 2863, 1675, 1596, 1463, 1276, 1197, 1164, 907; FAB *m/e* calcd for P + 1 ($C_{29}H_{44}NO_3Si$) 482.3092, observed *m/e* 482.3081.

***threo*-1-[4-[(Triisopropylsilyl)oxy]phenyl]-2-(4-hydroxy-4-phenylpiperidino)-1-propanol.** To a slurry of sodium borohydride (3.5 g, 0.92 mol) in ethanol (850 mL) was added 1-[4-[(triisopropylsilyl)oxy]phenyl]-2-(4-hydroxy-4-phenylpiperidino)-1-propanone (22.14 g, 46 mmol) in ethanol (250 mL) dropwise while monitoring that the pH of the solution was maintained at a pH of 7.5 or greater at all times. The mixture was allowed to stir overnight (24 h); then it was diluted with water and concentrated at reduced pressure. The residue was partitioned between ethyl acetate and water, the phases were separated, and the aqueous layer was extracted with ethyl acetate (2×). The combined organic layer was washed with brine, dried over calcium sulfate, and concentrated. Flash chromatography on silica gel, eluting with 25% and then 50% ethyl acetate/hexane, gave 15.4 g (69%), of *threo*-1-[4-[(triisopropylsilyl)oxy]phenyl]-2-(4-hydroxy-4-phenylpiperidino)-1-propanol as a white solid: mp 148–151 °C; NMR ($CDCl_3$) δ 7.52 (d, J = 7 Hz, 2 H), 7.38 (d, J = 7 Hz, 2 H), 7.30–7.25 (m, 1 H), 7.19 (d, J = 8.5 Hz, 2 H), 6.84 (d, J = 8.5 Hz, 2 H), 4.23 (d, J = 9.5 Hz, 1 H), 3.13–3.02 (m, 1 H), 2.80–2.58 (m, 3 H), 2.30–2.08 (m, 2 H), 1.90–1.78 (m, 2 H), 1.29–1.17 (m, 3 H), 1.09 (d, J = 7 Hz, 18 H), 0.79 (d, J = 6.5 Hz, 3 H); IR ($CHCl_3$) 3669 (w), 2943, 2863, 1608, 1504, 1265, 1199; FAB *m/e* P + 1 calcd for ($C_{29}H_{46}NO_3Si$) 484.3249, observed *m/e* 484.3256.

10: *threo*-1-[4-[(Triisopropylsilyl)oxy]phenyl]-2-(4-hydroxy-4-phenylpiperidino)-1-propanol (15.24 g, 31.6 mmol) was dissolved in tetrahydrofuran (500 mL), and 1 N tetrabutylammonium fluoride in THF (47.4 mL, 47.4 mmol) was added dropwise. The solution was stirred 45 min; then it was concentrated directly onto silica gel and flash chromatographed. Elution with 50% ethyl acetate/hexane followed by pure ethyl acetate gave 6.74 g (65%) of **10** as a white solid. A sample recrystallized from ethanol had the following properties: mp 202–204 °C; NMR (DMSO-d_6) δ 7.52 (d, J = 8 Hz, 2 H), 7.31 (t, J = 7.5 Hz, 2 H), 7.19 (d, J = 7 Hz, 1 H), 7.13 (d, J = 8 Hz, 2 H), 6.70 (d, J = 8.5 Hz, 2 H), 4.81 (s, 1 H), 4.16 (d, J = 9.5 Hz, 1 H), 3.45–3.41 (m, 1 H), 2.96 (t, J = 10.5 Hz, 1 H), 2.61–2.52 (m, 3 H), 2.00 (m, 1 H), 2.00–1.86 (m, 1 H), 1.64–1.61 (m, 2 H), 0.69 (d, J = 6.5 Hz, 3 H); IR (KBr) 2998, 1599, 1506, 1441, 1378, 1337, 1190, 1146, 1084, 1027, 1003. Anal. ($C_{20}H_{25}NO_3 \cdot 0.5C_2H_6O$) C, H, N.

5: mp 213–214 °C (ethyl acetate); NMR (DMSO-d_6) δ 7.25–7.11 (m, 5 H), 7.08 (d, J = 8.2 Hz, 2 H), 6.68 (d, J = 2 Hz, 2 H), 4.14 (s, 1 H), 4.09 (d, J = 9.2 Hz, 1 H), 3.33 (s, 2 H), 3.30 (s, 1 H), 2.74 (m, 1 H), 2.60–2.35 (m, 4 H), 1.70–1.40 (m, 4 H), 0.63 (d, J = 6.7 Hz, 3 H); IR (KBr) 3263, 3023, 2940, 2917, 1615, 1517, 1453, 1273, 1221, 1186, 1020, 1011, 831, 687. Anal. ($C_{21}H_{27}NO_3$) C, H, N.

6: mp 174–175 °C (toluene); NMR (dilute sample in $CDCl_3$) δ 7.47–7.13 (m, 7 H), 6.77 (d, J = 8.5 Hz, 2 H), 4.96 (br s, 1 H), 4.16 (d, J = 9.8 Hz, 1 H), 3.34 (s, 3 H), 2.88–2.73 (m, 1 H), 2.79 (s, 2 H), 2.62–2.33 (m, 4 H), 1.84–1.48 (m, 4 H), 0.75 (d, J = 6.5 Hz, 3 H). Anal. ($C_{22}H_{29}NO_3$) C, H, N.

7: mp 98–99 °C (ethanol); NMR (DMSO-d_6) δ 7.26–7.08 (m, 7 H), 6.68 (d, J = 8.5 Hz, 2 H), 4.56 (dd, J = 4, 8.8 Hz, 1 H), 4.17 (br s, 2 H), 2.65–2.27 (m with s at 2.65, 9 H), 1.59–

1.46 (m, 2 H), 1.37 (br d, J = 13 Hz, 2 H), IR (KBr) 3350, 2940, 2840, 1610, 1515, 1085, 835, 705. Anal. ($C_{20}H_{25}NO_3 \cdot H_2O$) C, H, N.

8: mp 190–191 °C (ethanol); NMR (methanol-d_4) δ 7.29–7.15 (m, 7 H), 6.74 (d, J = 8.4 Hz, 2 H), 4.13 (d, J = 9.5 Hz, 1 H), 3.10 (t, J = 10.4 Hz, 1 H), 2.76 (s, 2 H), 2.68–2.59 (m, 3 H), 2.48–2.41 (m, 1 H), 1.78–1.70 (m, 1 H), 1.63–1.53 (m, 4 H), 1.19–1.08 (m, 1 H), 0.64 (t, J = 7.5 Hz, 3 H); IR (KBr) 3250, 2935, 2910, 1610, 1515, 1445, 1260, 1230, 1165, 1035, 967, 849, 695. Anal. ($C_{22}H_{29}NO_3$) C, H, N.

9: mp 158–159 °C (ethanol/ether); NMR (methanol-d_4) δ 7.30–7.16 (m, 7 H), 6.75 (d, J = 8.5 Hz, 2 H), 4.15 (d, J = 9.8 Hz, 1 H), 3.07 (dt, J = 2.6, 11.4 Hz, 1 H), 2.76 (s, 2 H), 2.68–2.50 (m, 4 H), 1.74 (dt, J = 4.4, 10.1 Hz, 1 H), 1.64–1.50 (m, 4 H), 1.20–0.96 (m, 2 H), 0.94–0.82 (m, 1 H), 0.69 (t, J = 7 Hz, 3 H); IR (KBr) 3280, 2940, 2915, 1615, 1518, 1450, 1260, 840, 700, 620. Anal. ($C_{23}H_{31}NO_3$) C, H, N.

11: mp 200–201 °C (ethyl acetate); NMR (DMSO-d_6) δ 9.26 (br s, 1 H), 7.28–7.13 (m, 5 H), 7.10 (d, J = 8.5 Hz, 2 H), 6.69 (d, J = 8.5 Hz, 2 H), 4.92 (br s, 1 H), 4.13 (s, 1 H), 4.12 (d, J = 10 Hz, 1 H), 2.80 (br t, 1 H), 2.66–2.60 (m, 2 H), 2.49–2.35 (m, 3 H), 1.66–1.49 (m, 7 H), 0.66 (d, J = 6.5 Hz, 3 H); IR (KBr) 3320–3180 (br), 2925, 2910, 1620, 1520, 1455, 1415, 1265–1210 (br), 1190, 1170, 1155, 1135, 1120, 1030, 930, 840. Anal. ($C_{22}H_{29}NO_3$) C, H, N.

12: mp 200.5–201 °C (ethyl acetate); NMR (DMSO-d_6) δ 9.23 (br s, 1 H), 7.27–7.14 (m, 5 H), 7.09 (d, J = 8.5 Hz, 2 H), 6.68 (d, J = 8.5 Hz, 2 H), 4.85 (br s, 1 H), 4.09 (d, J = 9.5 Hz, 1 H), 3.96 (s, 1 H), 2.75 (br t, 1 H), 2.55 (t, J = 7.5 Hz, 2 H), 2.46–2.24 (m, 3 H), 1.68–1.34 (m, 9 H), 0.62 (d, J = 6.5 Hz, 3 H); IR (KBr) 3400–3180 (br), 2955, 1520, 1405, 1260, 1020, 1015, 935, 840. Anal. ($C_{23}H_{31}NO_3$) C, H, N.

13: mp 191–192 °C (ethanol); NMR ($CDCl_3$) δ 9.28 (br s, 1 H), 7.30–7.09 (m, 7 H), 6.69 (d, J = 8.5 Hz, 2 H), 4.85 (br s, 1 H), 4.11 (d, J = 9.5 Hz, 1 H), 3.94 (s, 1 H), 2.76–2.74 (m, 1 H), 2.58 (t, J = 7.5 Hz, 2 H), 2.50–2.35 (m, 3 H), 1.65–1.48 (m, 11 H), 0.65 (d, J = 6.5 Hz, 3 H); IR (KBr) 3300–3150 (br), 2940, 2910, 1520, 1465, 1270, 1245, 1230, 1180, 1170, 1025, 1015, 840. Anal. ($C_{24}H_{33}NO_3$) C, H, N.

14: mp 197–198 °C (ethyl acetate); NMR (DMSO-d_6) δ 9.22 (br s, 1 H), 7.54 (dd, J = 5.5, 9.0 Hz, 2 H), 7.14–7.09 (m, 4 H), 6.70 (d, J = 8.5 Hz, 2 H), 4.90 (br s, 1 H), 4.86 (s, 1 H), 4.15 (d, J = 9 Hz, 1 H), 2.94 (br t, J = 10.5 Hz, 1 H), 2.60–2.40 (m, 4 H), 2.07–1.91 (m, 2 H), 1.62–1.58 (m, 2 H), 0.67 (d, J = 6.5 Hz, 3 H); IR (KBr) 3400–3200 (br), 1515, 1260, 1240–1220 (br), 1165, 1150, 1045, 840. Anal. ($C_{20}H_{24}FNO_3$) C, H, N.

15: mp 204–206 °C (ethyl acetate); NMR (DMSO-d_6) δ 9.31 (s, 1 H), 7.57 (d, J = 8.5 Hz, 2 H), 7.38 (d, J = 8.5 Hz, 2 H), 7.14 (d, J = 8.5 Hz, 2 H), 6.72 (d, J = 8.5 Hz, 2 H), 4.95 (s, 2 H), 4.18 (d, J = 9.5 Hz, 1 H), 2.70–2.50 (m, 4 H), 2.46 (m, 1 H), 2.15–2.00 (m, 2 H), 1.68–1.50 (br d, 2 H), 0.70 (d, J = 6.5 Hz, 3 H); IR ($CHCl_3$) 3671 (w), 3584 (w), 2920, 1730, 1374, 1260–1190 (br). Anal. ($C_{20}H_{24}ClNO_3 \cdot 0.5H_2O$) C, H, N.

16: mp 188–189 °C (ethyl acetate); NMR (DMSO-d_6) δ 9.24 (br s, 1 H), 7.39 (d, J = 8 Hz, 2 H), 7.13–7.09 (m, 4 H), 6.69 (d, J = 8.5 Hz, 2 H), 4.97 (br s, 1 H), 4.72 (s, 1 H), 4.15 (d, J = 9.5 Hz, 1 H), 2.94 (br t, J = 10.5 Hz, 1 H), 2.58–2.40 (m, 4 H), 2.05–1.89 (m, 2 H), 1.62–1.58 (m, 2 H), 0.67 (d, J = 6.5 Hz, 3 H); IR (KBr) 3400–3300 (br), 1515, 1460, 1380, 1245, 1150, 1045, 915, 840, 830. Anal. ($C_{21}H_{27}NO_3$) C, H, N.

17: mp 149–152 °C (ethyl acetate/hexane); NMR ($CDCl_3$) δ 7.52–7.49 (m, 2 H), 7.39–7.24 (m, 8 H), 4.26 (d, J = 10 Hz, 1 H), 3.06 (dt, J = 2, 11.5 Hz, 1 H), 2.72–2.55 (m, 4 H), 2.27–2.07 (m, 2 H), 1.84–1.80 (m, 2 H), 1.71 (br s, 1 H), 0.82 (d, J = 6.5 Hz, 3 H); IR ($CHCl_3$) 2943, 2840, 1446, 1381, 1365, 1153, 1037, 1011. Anal. ($C_{20}H_{25}NO_2$) C, H, N.

18: mp 177–179 °C (ethanol); NMR ($CDCl_3$) δ 7.54–7.39 (m, 2 H), 7.40–7.25 (m, 5 H), 7.05–6.99 (m, 2 H), 4.27 (d, J = 9.5 Hz, 1 H), 3.13–3.05 (m, 1 H), 2.73–2.61 (m, 4 H), 2.29–2.03 (m, 2 H), 1.87–1.55 (m, 2 H), 0.83 (d, J = 6.5 Hz, 3 H); IR ($CHCl_3$) 3584 (w), 3309 (w), 2944, 2838, 1604, 1380, 1365, 1313, 1125, 1076, 1037, 1011, 830. Anal. ($C_{20}H_{24}FNO_2$) C, H, N.

19: mp 192–194 °C (ethyl acetate); NMR ($CDCl_3$) δ 7.53–7.49 (m, 2 H), 7.41–7.35 (m, 2 H), 7.30 (s, 5 H), 4.26 (d, J = 9.5 Hz, 1 H), 3.13–3.04 (m, 1 H), 2.73–2.58 (m, 4 H), 2.28–2.12 (m, 2 H), 1.87–1.82 (m, 2 H), 0.83 (d, J = 6.5 Hz, 3 H); IR ($CHCl_3$) 3582 (w), 3314 (w), 2941, 2838, 1489, 1396, 1381, 1366, 1314, 1152, 1080, 1038, 1011, 818. Anal. ($C_{20}H_{24}ClNO_2$) C, H, N.

20: mp 206.5–207 °C (tartrate, methanol), 203–204 °C (free base); NMR (free base, DMSO-d_6) δ 9.30 (br s, 1 H), 7.54 (d, J = 7.5 Hz, 2 H), 7.32 (t, J = 7.5 Hz, 2 H), 7.20 (t, J = 7 Hz, 1 H), 7.14 (d, J = 8.5 Hz, 2 H), 6.72 (d, J = 8.5 Hz, 2 H), 5.0 (br s, 1 H), 4.82 (s, 1 H), 4.17 (d, J = 9.5 Hz, 1 H), 3.38 (t, J = 10 Hz, 1 H), 2.64–2.40 (m, 4 H), 2.09 (dt, J = 4.5, 13 Hz, 1 H), 2.00–1.88 (m, 1 H), 1.64 (d, J = 12.5 Hz, 2 H), 0.70 (d, J = 6.5 Hz, 3 H); $[\alpha]^{22}_{Na}$ (tartrate) = +33.9°, c = 0.375 (water); $[\alpha]^{22}_{Na}$ (free base) = +56.9°, c = 0.26 (methanol). Anal. ($C_{20}H_{25}NO_3 \cdot C_4H_6O_6$) C, H, N.

21: mp and NMR are identical to **20**; $[\alpha]^{22}_{Na}$ (tartrate) = +36.2°, c = 0.375 (water); $[\alpha]^{22}_{Na}$ (free base) = −58.4°, c = 0.25 (methanol). Anal. ($C_{20}H_{25}NO_3 \cdot C_4H_6O_6$) C, H, N.

Blockade of NMDA-Induced Fos Expression. Male CF-1 mice (20–25 g) were used in this study. The mice were housed on a 12 h dark/light cycle at 22 °C with food and water available ad libitum. Test compounds were dissolved in 50% poly(ethylene glycol) and were administered ip 30 min before NMDA (75 mg/kg, a subseizure dose) was injected ip. One hour later, the mice were administered pentobarbital (80 mg/kg, ip) and then were perfused with 2% paraformaldehyde in 0.1 N phosphate-buffered saline (PBS) at pH 7.4. Brains were quickly dissected on ice and immersed in 2% paraformaldehyde/PBS for 1 h followed by overnight treatment with 15% sucrose in PBS. Brains were frozen on dry ice and stored at −80 °C until used. Two 50 μm coronal sections were taken from the hippocampal region of each brain using a cryostat and submerged in PBS in 24-well plates. The sections were washed with PBS (three times, 5 min per wash) and then incubated in a PBS solution containing 4% normal rabbit serum and 0.2% Triton X-100 for 1 h. The sections were then placed in a 1:1500 dilution of polyclonal antibody for Fos (Cambridge Research Inc., Sheep Anti-Fos, Catalog No. OA-11-823). The sections were again washed with PBS (three times, 5 min per wash) and incubated with biotinylated anti-sheep antibody (Vector Laboratories) for 2 h using a modification of the avidin–biotin technique as previously described.[24] The sections were again washed with PBS (three times, 5 min per wash); then they were incubated in Vector ABC solution and diluted as per the Vectastain protocol for 1 h at ambient temperature. The sections were again washed three times with PBS followed by treatment with reagents from a glucose oxidase substrate kit (Vector Laboratories) for approximately 20 min and washed once with water. Sections were mounted onto subbed slides, allowed to dry overnight, and then placed in 50%, 95%, and 100% ethanol (30 s exposure) and finally 100% xylene. Coverslips were then placed over mounting media for each slide and dried overnight. The intensity of staining of the dentate gyrus of each section was analyzed by a MCID analyzer (Imaging Research) using the relative optical density procedure. The ED_{50} was calculated comparing control (vehicle only) and total (NMDA only) sections. A "negative control" section was stained using the same protocol, but the fos antibody was incubated with blocking peptide OP-11-3210 (Cambridge Research Inc.) prior to use.

Supporting Information Available: X-ray structure determination data for the *p*-bromobenzyl ether of compound **21** (8 pages). Ordering information is given on any current masthead page.

References

(1) Rothman, S. M.; Olney, J. W. Excitotoxicity and the NMDA Receptor. *Trends Neurosci.* **1987**, *10*, 299–302 and references cited therein.

(2) Choi, D. W. Ionic Dependence of Glutamate Neurotoxicity. *J. Neurosci.* **1987**, *7*, 369–379 and references cited therein.

(3) DeFeudis, F. V. NMDA-Mediated Neurodegeneration and Cerebral Ischemia - Mechanisms and Therapeutic Perspectives. *Drugs Today* **1989**, *25*, 677–688. Choi, D. W. Cerebral Ischemia: Some New Approaches and Unanswered Questions. *J. Neurosci.* **1990**, *10*, 2493–2501.

(4) Greenamyre, J. T.; Penney, J. B.; D'Amato, C. J.; Young, A. B. Dementia of the Alzheimer's Type: Changes in Hippocampal L-[^{3}H]Glutamate Binding. *J. Neurochem.* **1987**, *48*, 543–551.

(5) Meldrum, B. Possible Therapeutic Applications of antagonists of Excitatory Amino Acid Neurotransmitters. *Clin. Sci.* **1985**, *68*, 113–122. Lehmann, J. The NMDA Receptor. *Drugs Future* **1989**, *14*, 1059–1071.
(6) Johnson, G. Recent Advances in Excitatory Amino Acid Research. *Annu. Rep. Med. Chem.* **1989**, *24*, 41–50. Johnson, G.; Bigge, C. F. Recent Advances in Excitatory Amino Acid Research. *Annu. Rep. Med. Chem.* **1991**, *26*, 11–22. Monn, J. A.; Schoepp, D. D. Recent Progress in Excitatory Amino Acid Research. *Annu. Rep. Med. Chem.* **1994**, *29*, 53–64.
(7) Scatton, B.; Carter, C.; Claustre, Y.; L'Heureux, R.; Arbilla, S.; Langer, S. Z.; Gotti, B.; Duverger, D.; MacKenzie, E. T. The Cerebral Anti-Ischemic Agents, Ifenprodil and SL-82.0715, Antagonise the Effects of NMDA. Proceedings of the Xth International Congress of Pharmacology, Sydney, Australia, Abstract No. 012.064, 1987.
(8) Carter, C.; Rivy, J.-P.; Scatton, B. Ifenprodil and SL-82.0715 Are Antagonists at the Polyamine Site of the N-Methyl-D-Aspartate (NMDA) Receptor. *Eur. J. Pharmacol.* **1989**, *164*, 611–612. Reynolds, I. J.; Miller, R. J. Ifenprodil is a Novel Type of N-Methyl-D-Aspartate Receptor Antagonist - Interaction with Polyamines. *Mol. Pharmacol.* **1989**, *36*, 758–765.
(9) Chenard, B. L.; Shalaby, I. A.; Koe, B. K.; Ronau, R. T.; Butler, T. W.; Prochniak, M. A.; Schmidt, A. W.; Fox, C. B. Separation of α1 Adrenergic and N-Methyl-D-Aspartate Antagonist Activity in a Series of Ifenprodil Compounds. *J. Med. Chem.* **1991**, *34*, 3085–3090.
(10) See ref 9 and Carron, C.; Jullien, A.; Bucher, B. Synthesis and Pharmacological Properties of a Series of 2-Piperidino Alkanol Derivatives. *Arzneim. Forsch.* **1971**, *21*, 1992–1998.
(11) All compounds have threo relative stereochemistry and are illustrated with a 1*S*,2*S* configuration. Compounds **1**–**19** are racemic. Compound **20** has a 1*S*,2*S* absolute configuration and compound **21** has a 1*R*,2*R* absolute configuration as determined by X-ray structure determination.
(12) Benzyl ethers are also perfectly suitable for protection of the phenol: unpublished work from our laboratory, but also see ref 10.
(13) Gaudillier, B.; Rousseau, J. European Patent 0 202 164 A1; *Chem. Abstr.* **1986**, *107*, 198088d. See also: Chenard, B. L.; Butler, T. W.; Shalaby, I. A.; Prochniak, M. A.; Koe, B. K; Fox, C. B. *Biomed. Chem. Lett.* **1993**, *3*, 91–94.
(14) Shalaby, I. A.; Chenard, B. L.; Prochniak, M. A.; Butler, T. W. Neuroprotective Effects of the N-Methyl-D-Aspartate Receptor Antagonists Ifenprodil and SL-82,0715 on Hippocampal Cells in Culture. *J. Pharmacol. Exp. Ther.* **1991**, *260*, 925–932. Also see: Choi, D.; Koh, J.-y.; Peters, S. Pharmacology of Glutamate Neurotoxicity in Cortical Cell Culture: Attenuation by NMDA Antagonists. *J. Neurosci.* **1988**, *8*, 185–196.
(15) We have previously shown that the neuroprotective effect of ifenprodil was not associated with its affinity for α_1 adrenergic or σ receptors; see ref 14.
(16) Greengrass, P.; Bremner, R. Binding Characteristics of Prazosin-H-3 to Rat-Brain Alpha-Adrenergic Receptors. *Eur. J. Pharmacol.* **1979**, *55*, 323–326.
(17) Gotte, B.; Duverger, D.; Bertin, J.; Carter, C.; Dupont, R.; Frost, J.; Baudilliere, B.; MacKenzie, E. T.; Rousseau, J.; Scatton, B.; Wick, A. Ifenprodil and SL 82.0715 as Cerebral Anti-Ischemic Agents. I. Evidence for Efficacy in Models of Focal Cerebral Ischemia. *J. Pharmacol. Exp. Ther.* **1988**, *247*, 1211–1221. Carter, C.; Benavides, J.; Legendre, P.; Vincent, J. D.; Noel, F.; Thuret, F.; Lloyd, K. G.; Arbilla, S.; Zivkovic, B.; MacKenzie, E. T.; Scatton, B.; Langer, S. Z. Ifenprodil and SL 82.0715 as Cerebral Anti-Ischemic Agents. II. Evidence for N-Methyl-D-Aspartate Receptor Antagonist Properties. *J. Pharmacol. Exp. Ther.* **1988**, *247*, 1222–1232. Carter, C. J.; Lloyd, K. G.; Zivkovic, B.; Scatton, B. Ifenprodil and SL 82.0715 as Cerebral Antiischemic Agents. III. Evidence for Antagonistic Effects at the Polyamine Modulatory Site Within the N-Methyl-D-Aspartate Receptor Complex. *J. Pharmacol. Exp. Ther.* **1990**, *253*, 475–482.
(18) We have also observed that relocation of the phenol hydroxyl group to the ortho or meta positions as well as replacement with bioisosteres such as amino, acetamido, sulfonamido similarly resulted in loss of NMDA antagonist activity (data not shown). Only cyclic bioisosteres such as oxindoles have yielded potent NMDA antagonists from the ifenprodil series. See: Chenard, B. L.; Butler, T. W.; Shalaby, I. A.; Prochniak, M. A.; Koe, B. K.; Fox, C. B. Oxindole N-Methyl-D-Aspartate (NMDA) Antagonists. *Biomed. Chem. Lett.* **1993**, *3*, 91–94. Frost, J.; Lardenois, P. European Patent Application EP 481853-A.
(19) Coupling of ifenprodil's actions at the NMDA receptor to the polyamine modulatory site may be sensitive to the particular neurons examined in culture (cortex versus hippocampus). See: Tamura, Y.; Sato, Y.; Yokota, T.; Akaike, A.; Sasa, M.; Takaori, S. Ifenprodil Prevents Glutamate Cytotoxicity via Polyamine Modulatory Sites of N-Methyl-D-Aspartate Receptors in Cultured Cortical Neurons. *J. Pharmacol. Exp. Ther.* **1993**, *265*, 1017–1025.
(20) Column: Ultron ES-OVM, Shinwa Chemical Industries. Mobile phase: 10/90 (v/v) acetonitrile/0.01 M aqueous KH_2PO_4, pH 6.5. Flow rate: 1 mL/min. Detection: UV at 226 nM. Column temperature: 40 °C. Approximate retention times: **21** (6.15 min) and **20** (8.14 min).
(21) Schmidt, W. J.; Bubser, M. Anticataleptic Effects of the N-Methyl-D-Aspartate Antagonist MK-801 in Rats. *Pharmacol. Biochem. Behavior* **1989**, *32*, 621–623. Mehta, A. K.; Ticku, M. K. Role of N-Methyl-D-Aspartate (NMDA) Receptors in Experimental Catalepsy in Rats. *Life Sci.* **1990**, *46*, 37–42.
(22) Sheng, M.; Greenberg, M. E. The Regulation and Function of c-fos and Other Immediate Early Genes in the Nervous System. *Neuron* **1990**, *4*, 477–485.
(23) Dragunow, M.; Faull, R. L. M.; Jansen, K. L. R. MK-801, an Antagonist of NMDA Receptors, Inhibits injury-Induced c-fos accumulation in Rat Brain. *Neurosci. Lett.* **1990**, *109*, 128–133.
(24) Popovici, T.; Barbin, G.; Ben-Ari, Y. Kainic Acid Induced Seizures Increase c-fos-like Protein in the Hippocamups. *Eur. J. Pharmacol.* **1988**, *150*, 405–406. Popovici, T.; Represa, A.; Crepel, V.; Barbin, G.; Beaudoin, M.; Ben-Ari, Y. Effects of Kainic Acid-Induced Seizures and Ischemia on c-fos-like Proteins in Rat Brain. *Brain Res.* **1990**, *536*, 183–194.
(25) Sonnenberg, J. L.; Mitchelmore, C.; Macgregor-Leon, P. F.; Hempstead, J.; Morgan, J. I.; Curran, T. Glutamate Receptor Agonists Increase the Expression of Fos, Fra, and AP-1 DNA Binding Activity in the Mammalian Brain. *J. Neurosci. Res.* **1989**, *24*, 72–80. Le, F.; Wilce, P. A.; Hume, D. A.; Shanley, B. C. Involvement of g-Aminobutyric Acid and N-Methyl-D-Aspartate Receptors in the Inhibitory Effect of Ethanol on Pentylenetetrazole-Induced c-fos Expression in Rat Brain. *J. Neurochem.* **1992**, *59*, 1309–1315.
(26) Sharp, J. W.; Sagar, S. M.; Hisanaga, K.; Jasper, P.; Sharp, F. R. The NMDA Receptor Mediates Cortical Induction of fos and fos-Related Antigens Following Cortical Injury. *Exp. Neurol.* **1990**, *109*, 323–332.
(27) Drug metabolism studies with **20** and **21** showed that brain exposure was essentially equivalent for both following equivalent doses in rat iv. (Data from the laboratory of Dr. J. G. Baxter which will be published elsewhere.)
(28) Neuronal vacuolization: Olney, J. W.; Labruyere, J.; Price, M. T. Pathological Changes Induced in Cerebrocortical Neurons by Phencyclidine and Related Drugs. *Science* **1989**, *244*, 1360–1362. Stimulant effects: Clineschmidt, B. V.; Martin, G. E.; Bunting, P. R.; Papp, N. L. Central Sympathomimetic Activity of Dextro-5-Methyl-10,11-dihydro-5H-dibenzo-A-D-cyclohepten-5,10-imine MK-801: A Substance with Potent Anticonvulsant Central Sympathomimetic and Apparent Anxiolytic Properties. *Drug Dev. Res.* **1982**, *2*, 135–146. Psychotomimetic effects: Snyder, S. H. Phencyclidine. *Nature* **1980**, *285*, 355–356; Zukin, R. S.; Zukin, S. R. Demonstration of [^{3}H] Cyclazocine Binding to Multiple Opiate Receptor-Sites. *Mol. Pharmacol.* **1981**, *20*, 246–254. Blood-brain penetration question for a competitive NMDA antagonist: Hogan, M. J.; Gjedde, A.; Hakim, A. M. In Vivo Distribution of CGS-19755 within Brain in a Model of Focal Cerebral Ischemia. *J. Neurosci.* **1992**, *58*, 186–191.
(29) We have observed that a two-atom spacer between the C-4 phenyl group and the piperidine ring consistently enhances α_1 adrenergic binding affinity relative to the corresponding homologs with longer or shorter tethers or the directly attached C-4 phenyl group in other series as well. Unpublished data from our laboratories.
(30) For leading references to the isolation and characterization of NMDA receptors, see: Ishii, T.; Moriyoshi, K.; Sugihara, H.; Sakurada, K.; Kadotani, H.; Yokoi, M.; Akazawa, C.; Shigemoto, R.; Mizuno, N.; Masu, M.; Nakanishi, S. Molecular Characterization of the Family of the N-Methyl-D-Aspartate Receptor Subunits. *J. Biol. Chem.* **1993**, *268*, 2836–2843. Seeburg, P. H. The Molecular Biology of Mammalian Glutamate Receptor Channels *Trends Neurosci.* **1993**, *16*, 359–365.
(31) Monyer, H.; Sprengel, R.; Schoepfer, R.; Herb, A.; Higuchi, M.; Lomeli, H.; Burnashev, N.; Sakmann, B.; Seeburg, P. Heteromeric NMDA Receptors: Molecular and Functional Distinction of Subtypes. *Science* **1992**, *256*, 1217–1221.
(32) Williams, K.; Russell, S. L.; Shen, Y. M.; Molinoff, P. B. Developmental Switch in the Expression of NMDA Receptors Occurs In Vivo and In Vitro. *Neuron* **1993**, *10*, 267–278.
(33) Manuscripts in preparation.

JM950231U